ULTRAHIGH RESOLUTION LITHOGRAPHY WITH EXCIMER LASERS

F.K. TITTEL, M. ERDÉLYI*, C. SENGUPTA, ZS. BOR*,
G. SZABÓ*, J.R. CAVALLARO, M.C. SMAYLING, W.L. WILSON
Department of Electrical & Computer Engineering and Rice Quantum Institute, Rice University, P.O. Box 1892, Houston, TX 77251, USA
**Department of Optics and Quantum Electronics, JATE University, Dóm tér 9, H-6720 Szeged, Hungary*

1. Introduction

The photolithography process is central to integrated circuit fabrication. Through this process an integrated circuit is patterned by imaging a photomask onto a layer of photoresist. The light source currently being used by the semiconductor industry in the photolithographic process for 0.35 micron feature size is the mercury lamp. This light source has wavelengths of 436 nanometers (g-line) and 365 nanometers (i-line). As the feature size for integrated circuits moves below 0.35 microns, a new source of shorter wavelength light and higher power must be found to replace the mercury lamp. Excimer lasers are capable of producing wavelengths at 248 nanometers and 193 nanometers which could allow for design features down to 0.18 microns. Accordingly, as mercury lamp technology reaches its limits with the introduction of the "shrink" version of the 64 megabit DRAM (0.32 micron) and advanced microprocessors, the semiconductor industry will shift to excimer DUV lithography starting in ~1996. Furthermore, higher performance integrated circuits will require improved spatial resolution, larger projection areas, and higher throughput lithographic strategies. Wavefront enhancement technologies such as phase shift masks and/or off axis illumination will play an important role in these new generations of integrated circuits.

Since deep-UV lithography was first demonstrated using KrF excimer lasers, [1,2] the performance and reliability of these deep UV light sources have continuously improved. Current excimer laser models satisfy the optical specification and uptime requirements necessary for pilot integrated circuit production. Attention has now been focused on the Cost of Ownership (CoO) for these excimer laser light sources. Both line-narrowed KrF lasers for stepper/scanner systems and broadband KrF lasers for scanner systems must achieve reductions in CoO in order to compete on cost basis with I-line steppers using phase shifting masks or non-conventional illumination schemes.

The key technological needs for excimer lasers in microlithography are: 1) lowered operating costs (longer chamber lifetimes, lower gas consumption); 2) higher repetition rates ($> =$ 1000 Hz) for scanned exposures; 3) improved pulse to pulse energy repeatability; and 4) both line-narrowed (refractive lenses) and broadband (reflective/catidioptic) optics.

As feature size shrinks, there are two choices for decreasing the resolvable linewidth, W. From the relationship

$$W = k_1 \frac{\lambda}{NA} \tag{1}$$

where λ is the illumination wavelength, NA is the numerical aperture of the optical system, and k_1 is a system dependent parameter. It is obvious that a smaller W can result from either a reduction of the illumination wavelength λ or a larger imaging system numerical aperture, NA. The desire for shorter wavelengths will lead to the adoption of excimer lasers (KrF and ArF) as high brightness UV illumination sources. Achieving a larger numerical aperture is a challenge and is one of the reasons for the high cost of modern photolithographic steppers. The depth of focus (DOF) is given by

$$DOF = k_2 \frac{\lambda}{NA^2} . \tag{2}$$

Thus, decreasing λ and increasing the NA cause a serious degradation to the depth of focus and, consequently, the final image at the wafer. In particular, the inverse square relationship between DOF and NA is a serious problem. A smaller DOF requires a more stable and controlled, and hence costlier, stepper. The problem of reduced DOF becomes important as the surface of the fabricated wafer becomes increasingly non-planar as process steps increase in complexity.

An alternate approach to decreased W and increased DOF is to alter the optical system coefficients k_1 and k_2. One technique that has been shown to significantly improve both resolution limit and depth of field of the photolithographic image is that of phase shifting [4-6]. By appropriate optical manipulation, the electric field of adjacent regions of the photolithographic image can be made to be 180° out of phase with one another. This assures that when these images overlap (due to diffraction) there will be some place where the two images exactly cancel one another, resulting in near 100% contrast. The desired phase shift is usually accomplished by making some regions of the photolithographic mask optically thicker than in other regions. This is achieved by either etching regions of the mask, or by adding an additional layer to the mask, and then etching it away from unwanted regions. The finished mask and the resultant image at the silicon wafer surface are shown schematically in Figure 1. Besides the alternating phase-shift regions mentioned above, phase-shift regions can be placed at the rim of larger structures to enhance the contrast of their image. More recently, chromeless phase shift masks [6], as well as attenuating masks which achieve the desired

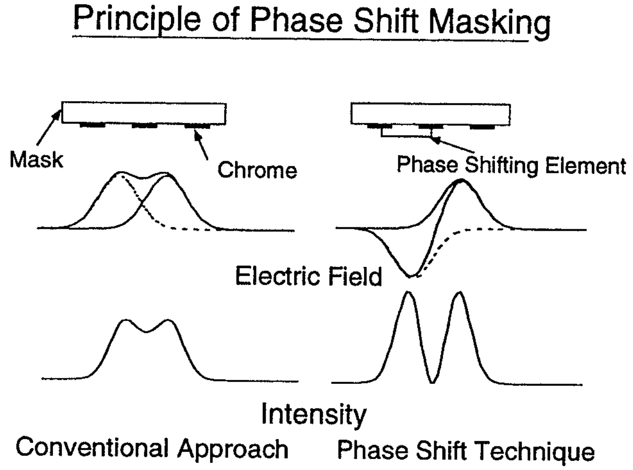

Figure 1: Comparison of Conventional and Phase-Shift Masking

phase shift effect by propagating some of the light through lossy regions in the mask, have been studied [7,8].

While any of these approaches to phase shifting have shown significant promise and offer distinct advantages over conventional photolithography, implementing the phase shifting technique to deep UV wavelengths requires tighter tolerances for the appropriate phase shift material as the wavelength is decreased. It is also much harder to find appropriate phase shifting materials which do not absorb strongly in the DUV region.

Recently, we reported progress on a novel phase shifting technique which does not require special phase shifting regions built into the mask [9-11]. By using a reflective chrome mask in a laser-based interferometric scheme, the desired phase shift can be achieved.

As outlined in Figure 2, light from a laser is divided into two beams by a beam splitter. One beam passes through the mask, while the other is reflected off the back of the mask. The two beams are then imaged onto the wafer surface. The optical path lengths of the two beams are adjusted so that their relative phase is 180° apart and the desired phase-shift effect is achieved. With this technique, we have demonstrated that it is possible to write line and space patterns with a linewidth of less than 0.3 μm using a frequency tripled Nd:YAG laser at 355 nm as the illumination source. CCD camera imaging, as well as computer simulations, obtained using DEPICT [12], show the effectiveness of this new scheme, as shown in Figure 3. One of the unique features of this approach is that both the amplitude and the phase of the two incident images are independently adjustable even after mask fabrication, which is not the case for most other phase shifting techniques.

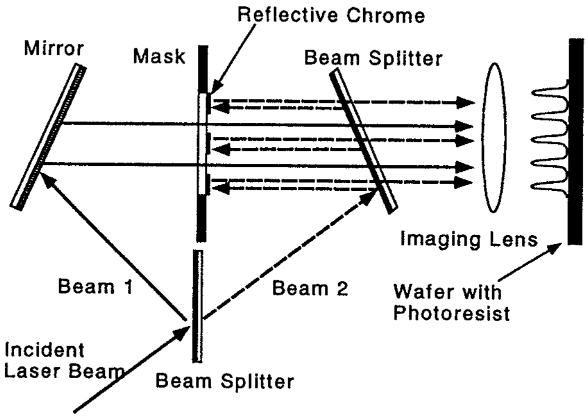

Figure 2: Interferometric Phase-Shift Technique

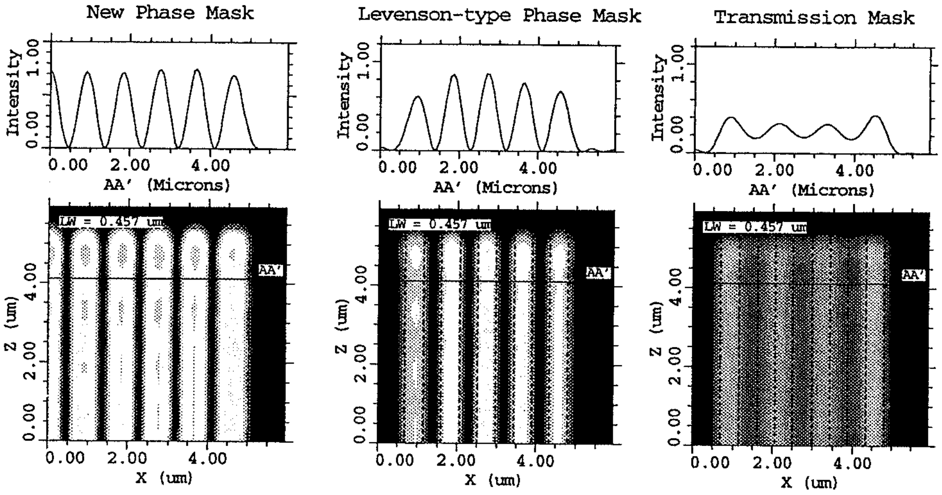
New Phase Mask

Levenson-type Phase Mask

Transmission Mask

Figure 3: Simulation results for the interferometric phase-shift method, Levenson-type phase-shift mask and transmission mask

In this paper we report on recent investigations where the interferometric technique described above is combined with off-axis illumination [13]. The ability to independently control the amplitude of the two out-of-phase beams is especially helpful in this application. Improved resolution, as well as greater depth of focus, result from applying this new imaging scheme.

Phase shifting can increase the depth of focus by about 50%. Off-axis illumination can add an additional 40% of depth of focus [14]. However, since off-axis illumination uses the first order diffracted beam (amplitude $\frac{1}{\pi}$) instead of the principal or zero order beam (amplitude $\frac{1}{2}$), the image contrast is reduced by about 5%. The additional use of an attenuated phase shift mask with a transmission of about 5% can compensate for this, however, and the equalized intensity can result in a 100% image contrast [15].

2. Experimental Set-Up

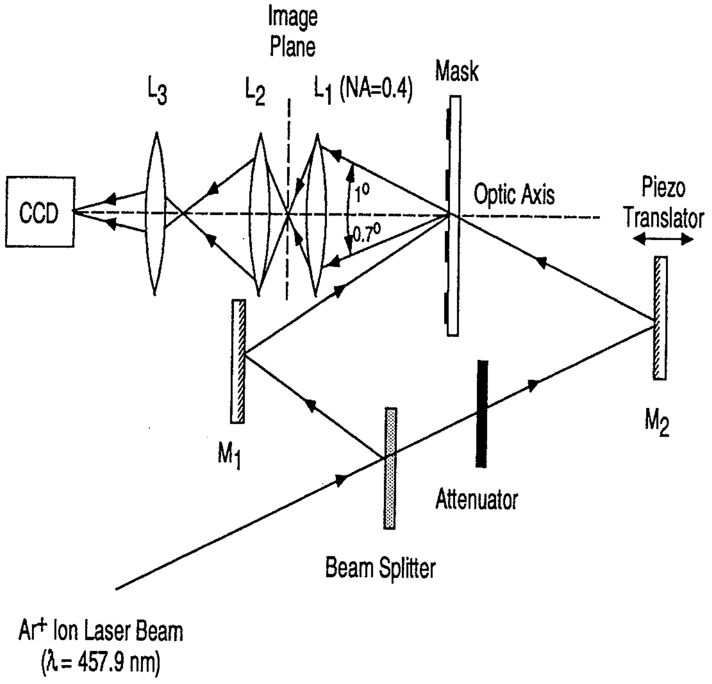

Figure 4: Experimental scheme of the off-axis illumination, combined with interferometric phase shifting. The mask is illuminated symmetrically from both sides with a beam splitter and two mirrors (M_1, M_2).

Figure 4 shows the experimental arrangement. The mask was a patterned evaporated, reflective chrome layer on fused silica substrate, forming a line and space pattern, with a spatial frequency of 16 μm.

The output from an Ar^+ laser beam operating at 457.9 nm was split into two beams and used to illuminate both the front and back surface of the mask. The intensity and the phase of the back illumination was controlled by a variable attenuator and a piezo-controlled linear translator, respectively. A microscope objective (magnification (M) = 20X, NA = 0.4) was used to image the mask onto the photoresist. The mask to objective distance was adjusted to the microscope tube length to ensure a nominal magnification ratio of 20X and high image quality. The off-axis illumination angle of the mask was 1° and the first order diffraction angle was 0.7° while all other diffraction orders were rejected by the aperture of the lens. The image of the line-space patterns formed by the lens L1 was magnified with two microscope objectives, L2 and L3, in tandem (M = 20X, NA = 0.5, and M = 40X, NA = 0.65). Special care was taken to avoid any optical degradation of the image by lenses L2 and L3. The imaging lens L2 was mounted on a precision translator to measure the depth of focus of the image. The magnified image was projected by lenses L2 and L3 onto a CCD camera.

3. Experimental Results

The performance of the new scheme was evaluated by two different methods. In the first the image was evaluated by CCD camera measurements of the image. The second method of evaluation consisted of making actual patterns in photoresist and then observing them using either a scanning electron microscope or an atomic force microscope.

The experimental results using the CCD camera, along with calculated simulation results, are shown in Figure 5. Figure 5.1a shows the results obtained with only the front of the mask illuminated. The simulation (5.1b) predicts a contrast ratio C

$$C = \frac{I_{max} - I_{min}}{I_{max} + I_{min}} \tag{3}$$

of about 90%, taking into account the zero and first order diffracted beams from an equal lines-and-space pattern. However, the simulator assumes perfect reflectivity for the chrome layer and ignores the dielectric reflection from the clear regions of the mask. Taking these into account (chrome reflectivity $R_{chrome} = 0.7$ and mask reflectivity $R_{mask} = 0.032$), the calculated image contrast decreases to about 67%, as compared to the 69% measured in this experiment.

Figure 5.2a shows the image of the mask when the front reflected beam was blocked and only the transmitted beams were intercepted by the imaging microscope lens L1. A careful comparison of Figure 5.1a and 5.2a shows (see the vertical dotted lines), that these images are spatially shifted by half the period of the pattern. This means that there is no transmission from the back side, where there is a reflection from the front side of the mask (see Figure 4).

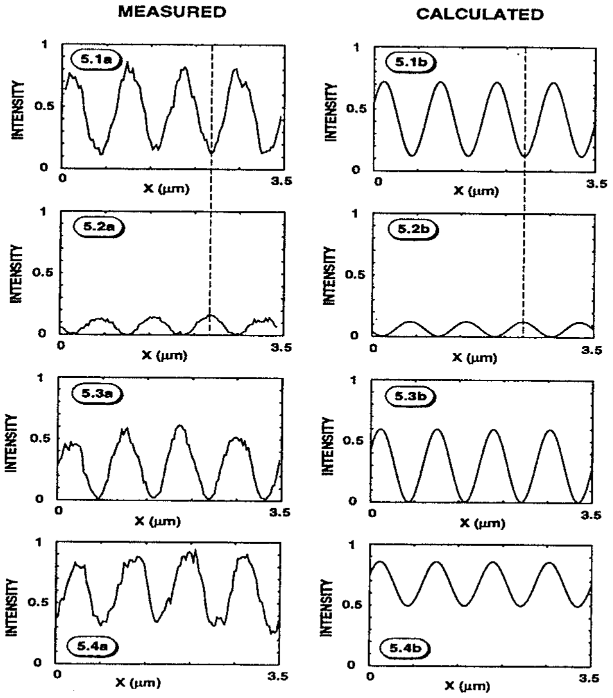

Figure 5: Intensity patterns obtained by the CCD camera. The (a) figures show the measured and the (b) figures show the calculated curves. 5.1: blocking the back illumination; 5.2: blocking the front illumination; 5.3: using both beams with 180° phase difference; 5.4: using both beams with 0° phase difference on the surface of the mask.

Figure 5.3a shows the interference pattern, when both beams were used and the phase of the transmitted image was shifted by π with respect to the reflected image, using the piezo-controlled translator of mirror M2. The intensity of the transmitted beam was adjusted with the attenuator shown in Figure 4, so that the peak intensity of the transmitted pattern was equal to the minimum intensity of the reflected pattern (see Figures 5.1a and 5.2a). Due to the π phase shift of the patterns, the electric fields are subtracted, resulting in a nearly 100% modulation depth of the image. Due to the high spatial coherence of the illuminating laser beam, the high contrast of the image remains for almost a 5 μm defocus in either direction. When the phase shift between the transmitted and reflected images is set to 0 or multiples of 2π, the electric fields of the two beams are added and the visibility decreases (Figure 5.4a) significantly.

The image of the line-space patterns was also recorded in a photoresist (Shipley 94314) using the off-axis-phase shifted scheme, with the 457.8 nm Ar^+ ion laser line. An atomic force microscope image of an exposed photoresist is shown in Figure 6. A feature size of 0.4 μm in the image plane can be calculated, knowing the period of the line-space pattern on the mask and the magnification of the objective L1. This value agrees well with the period of the exposed pattern.

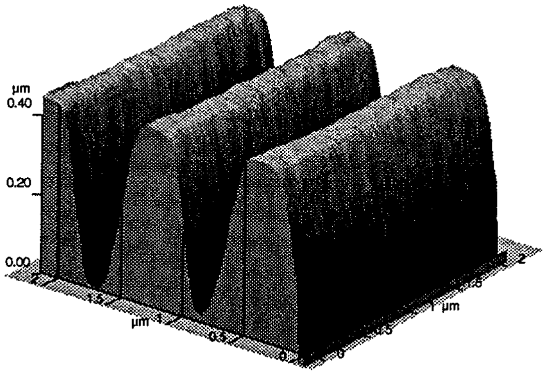

Figure 6: AFM image of patterns produced on the photoresist.

4. Conclusions

The feasibility of a new high resolution photolithography scheme combining off-axis illumination with interferometric phase shifting was demonstrated. Using a laser operating at 457.9 nm, feature sizes of 0.4 μm were obtained with a DOF of 10 μm. Because of the freedom to adjust the relative phase and amplitude of the two illuminating beams, the modulation depth could be improved to almost 100%. This freedom of adjustment makes this scheme a useful test bed for studying various phase shifting and off-axis illumination schemes.

5. Acknowledgment

This research was supported in part by NSF under grant DDM-9202639 and NSF-INT 9020541.

6. References

1. Pol V. et al (1986) Excimer laser-based lithography: A deep ultraviolet wafer stepper, *Proceedings of Optical/Laser Microlithography* **Vol. 633**, SPIE, 6-16.

2. Partlo W. N., Sandstrom R. L., Fomenkov I. V., and Das P. P. (1995) Low cost of ownership KrF excimer laser using a novel pulse power and chamber configuration, *Proceedings of Optical/Laser Microlithography VIII* **Vol. 2440**, SPIE.

3. Pätzel, R., Kleinschmidt, J., Rebhan, U., Franklin, J., and Endert, H. (1995) KrF Excimer Laser with repetition rates of 1 kHz for DUV Lithography, *Proceedings of Optical/Laser Microlithography VIII* **Vol. 2440**, SPIE.

4. Levenson, M.D. and Visnawathan, N.S. (1982) Improving resolution in photolithography with phase-shifting mask, *IEEE Trans. Elec. Devices* **ED-29**, 1828-1836.

5. Lin, B.J. (1993) Phase-shifting masks gain an edge, *IEEE Circuits and Devices* **2**, 28-35.

6. Toh, K., Dao, G., Singh, R., and Gaw, H. (1990) A chromeless phase-shifted mask: A new approach to phase-shifting masks, *Proceedings of 10th Annual Symposium on Microlithography* **Vol. 1496**, SPIE, 27-53.

7. Nakajima, M., Yoshioka, N., Miyzaki, J., Kusnose, H., Hosono, K., Morimoto, H., Watakabe, Y., and Tsukamoto, K. (1994) Attenuated phase-shift mask with a single layer absorptive shifter of CrO, CrON, MoSiO, and MoSiON film, *Proceedings of Optical/Laser Microlithography VII* **Vol. 2197**, SPIE, San Jose, CA, 111-121.

8. Wong, A., Pierrat, C., Vasdev, P., and Neureuther, A. (1994) Phase-shifter edge effect on attenuated phase-shifting mask image quality, *Proceedings of Optical/Laser Microlithography VII* **Vol. 2197**, SPIE, San Jose, CA, 122-129.

9. Kido, M., Szabó, G., Cavallaro, J. R., Wilson, W. L., and Tittel, F. K. (1994) A new phase shifting method for high resolution microlithography, *Proceedings of Optical/Laser Microlithography VII* **Vol. 2197**, SPIE, San Jose, CA, 835-843.

10. Tittel, F.K., Cavallaro, J. R., Kido, M., Smayling M. C., Szabó, G. and Wilson, W. L. (1995) Interferometric phase shift technique for high resolution microlithography, *Proceedings of 10th Int'l Symposium on Gas Flow and Chemical Lasers* **Vol. 2502**, SPIE, 617-624.

11. Kido, M., Szabó, G., Cavallaro, J. R., Wilson, W. L., Smayling, M. C., and Tittel, F. K. (1995) Submicron Optical Lithography Based on a New Interferometric Phase Shifting Technique, *Jpn. J. Appl. Phys.* **34**, 43-47.

12. Pack, R., and Bernard, D. (1990) *DEPICT-2 applications for VLSI technology*, Technology Modeling Associates, Palo Alto, CA.

13. Erdélyi M., Sengupta C., Bor Z., Cavallaro J. R., Kido M., Smayling M. C., Tittel F. K., Wilson W. L. and Szabó G. (1995) A new interferometric phase-shifting technique for sub-half-micron laser microlithography, *Proceedings of Optical/Laser Microlithography VIII* **Vol. 2440**, SPIE, 827-837.

14. Luehrmann, P., Oorschot, P.V., Jasper, H., Stalnaker, S., Brainerd, B., Rolfson, R., and Karklin, L. (1993) 0.35 μm lithography using off-axis illumination, *Proceedings of Optical/Laser Microlithography VII* **Vol. 1927**, SPIE, 103-124.

15. Fukuda, H., Imai, A., Terasawa, T., and Okazaki, S. (1991) New approach to resolution limit and advanced image formation techniques in optical lithography, *IEEE Trans. Elec. Devices* **ED-38**, 67-75.